

# Position-controlled quantum emitters with reproducible emission wavelength in hexagonal boron nitride

Clarisse Fournier<sup>1</sup>, Alexandre Plaud<sup>1</sup>, Sébastien Roux<sup>1</sup>, Aurélie Pierret<sup>2</sup>,  
Michael Rosticher<sup>2</sup>, Kenji Watanabe<sup>3</sup>, Takashi Taniguchi<sup>4</sup>, Stéphanie Buil<sup>1</sup>,  
Xavier Quélin<sup>1</sup>, Julien Barjon<sup>1</sup>, Jean-Pierre Hermier<sup>1</sup> and Aymeric Delteil<sup>1,\*</sup>

<sup>1</sup> *Université Paris-Saclay, UVSQ, CNRS, GEMaC, 78000, Versailles, France.*

<sup>2</sup> *Laboratoire de Physique de l'École Normale Supérieure, ENS, Université  
PSL, CNRS, Sorbonne Université, Université de Paris, 75005 Paris, France*

<sup>3</sup> *Research Center for Functional Materials, National Institute  
for Materials Science, 1-1 Namiki, Tsukuba 305-0044, Japan*

<sup>4</sup> *International Center for Materials Nanoarchitectonics, National  
Institute for Materials Science, 1-1 Namiki, Tsukuba 305-0044, Japan*

\* e-mail: [aymeric.delteil@uvsq.fr](mailto:aymeric.delteil@uvsq.fr)

Single photon emitters (SPEs) in low-dimensional layered materials have recently gained a large interest [1–4] owing to the auspicious perspectives of integration and extreme miniaturization offered by this class of materials [5]. However, accurate control of both the spatial location and the emission wavelength of the quantum emitters is essentially lacking to date [6], thus hindering further technological steps towards scalable quantum photonic devices [7]. Here, we evidence SPEs in high purity synthetic hexagonal boron nitride (hBN) that can be activated by an electron beam at chosen locations, with a spatial accuracy better than the cubed emission wavelength. Stable and bright single photon emission is subsequently observed in the visible range up to room temperature upon non-resonant laser excitation. Moreover, the low-temperature emission wavelength is reproducible within a range of 5 meV, a statistical dispersion that is more than one order of magnitude lower than the narrowest wavelength spreads obtained in epitaxial hBN samples [8, 9]. Our findings constitute an essential step towards the realization of top-down integrated devices based on identical quantum emitters in 2D materials.

The technological control of van der Waals materials is continually expanding, motivated by the

possibility of realizing increasingly complex hetero- and nanostructures of minimal thickness. The considerable variety of impacted fields of physics [10, 11] has been including solid-state quantum optics [12] since the discovery of single photon emission in WSe<sub>2</sub> [13–16] and hBN [17]. In the latter material, quantum emission is associated with point defects that were long thought to be of the intrinsic kind, although carbon impurities have been shown to play a role in the structure of at least part of the observed SPEs [8]. Their emission is found to be bright, stable [20, 21] and spectrally narrow [22, 23], and persists up to room temperature and above [24]. They however suffer from large discrepancies between their emission wavelengths, which are typically found between 550 and 850 nm [6, 25]. Epitaxial hBN grown by chemical vapour epitaxy has been recently shown to lead to a narrowing of the spectral distribution down to about 20 nm (75 meV) around a centre wavelength of 585 nm [8, 9]. Moreover, the SPEs appear in most cases at random locations in the crystal, although often preferentially close to the flake edges [26]. Effort towards controlling their position has included the use of focused ion beam [27], as well as strain through exfoliation on patterned substrates [28], but the emitters obtained with these methods exhibit large variations in their number, emission wavelength and optical properties. Moreover, the latter method results in limited possibilities of subsequent integration.

Here, we demonstrate the activation of colour centres at chosen locations using the electron beam of a commercial scanning electron microscope (SEM). Electron irradiation has already been shown to increase the formation probability of the SPEs [25, 26, 29], but to date has never been the basis of a process that allows to activate SPEs at preselected locations. We use high purity hBN synthesized at high pressure, high temperature (HPHT) [30], of which we exfoliate single flakes of a few tens of nanometres thickness on a silicon substrate, either with or without a top 285 nm SiO<sub>2</sub> layer. The flakes are irradiated using an electron beam of 15 keV acceleration voltage, under a current of 10 nA. The beam is adjusted to be about 330 nm diameter, to compromise between maximizing both the interaction cross-section and the localization accuracy. The irradiation time used in the first part of this work is fixed at 1000 s per irradiated spot. No additional treatment is performed to the sample. After the irradiation process, the sample is subsequently characterized in photoluminescence (PL) in a confocal microscope, either at room temperature or at cryogenic temperature down to 5 K. The SPEs are non-resonantly excited using a laser at 405 nm, in pulsed or continuous wave regime. Fig. 1a shows a SEM image of one of the irradiated flakes (of thickness 60 nm), together with a low temperature (5 K) confocal fluorescence map of the irradiated zone

(Fig. 1b). Emission from ensembles of colour centres is observed in all irradiated spots, within a radius close to that of the electron beam (see Supplementary Information) and thus showing that the emitters are localized in a volume of about  $3.5 \cdot 10^{-2} \mu\text{m}^3 \approx 0.4\lambda^3$ , where  $\lambda \approx 435 \text{ nm}$  is the emission wavelength. The low-temperature spectra associated with the irradiated sites are shown Fig. 1c and d with two different resolutions. On the coarse resolution spectra (Fig. 1c), the overall common spectral shape of the SPEs can be observed: they exhibit a sharp zero-phonon line (ZPL) around 2.846 eV (435.7 nm) that concentrates about 40 % of the light emission, as well as an adjacent acoustic phonon sideband (45 %) and a two-maxima optical phonon replica  $\sim 160 \text{ meV}$  away (15 %), which is typical of quantum emitters in hBN. The high resolution spectra, centred around the ZPL, is shown Fig. 1d, where ensembles of discrete lines are observed. Keeping the above-mentioned irradiation parameters, we have overall realized 26 irradiation spots on 3 flakes. All of them gave rise to small ensembles of similar emission wavelength, with ZPLs found within 5 meV (0.7 nm) around 435.7 nm, corresponding to an ensemble inhomogeneous linewidth (full width at half maximum, FWHM) of 1.7 meV (0.26 nm). We estimate the number of emitters per site to be of order of a few tens, as confirmed by photon correlation measurements. Remarkably, no colour centre, neither at 435 nm nor in the more usual wavelength range 550-850 nm, has been observed elsewhere on the flakes, although broad emission can be measured near the edges or close to flake defects. Interestingly, we note that light emission around 435 nm has already been observed in hBN as reported by Shevitski *et al.* [31]. In the latter work however, blue emission could solely be observed in cathodoluminescence and did neither respond to laser excitation, nor exhibit any antibunching behaviour in the photon statistics. Nonetheless, it is likely that the SPEs we report here are of the same nature – we presume that, in our case, we are able to activate the response of the emitters to photoluminescence owing to our electron irradiation parameters being very different from those used in [31], where the electron irradiation dose is several orders of magnitude smaller. We also mention that our irradiation procedure did not lead to SPE activation in other sources of hBN grown at atmospheric pressure, consistently with Shevitski *et al.* [31], suggesting a physical origin of the SPEs related either to the HPHT growth conditions or to the specific solvent precursor used during the hBN synthesis.

In order to investigate the individual properties of the colour centres, we have performed additional irradiations with a reduced exposition time (either 300 or 600 s) and a slightly larger electron beam ( $\sim 1 \mu\text{m}$  diameter) on a thinner flake ( $\sim 30 \text{ nm}$  thickness). The irradiations yielded SPEs,

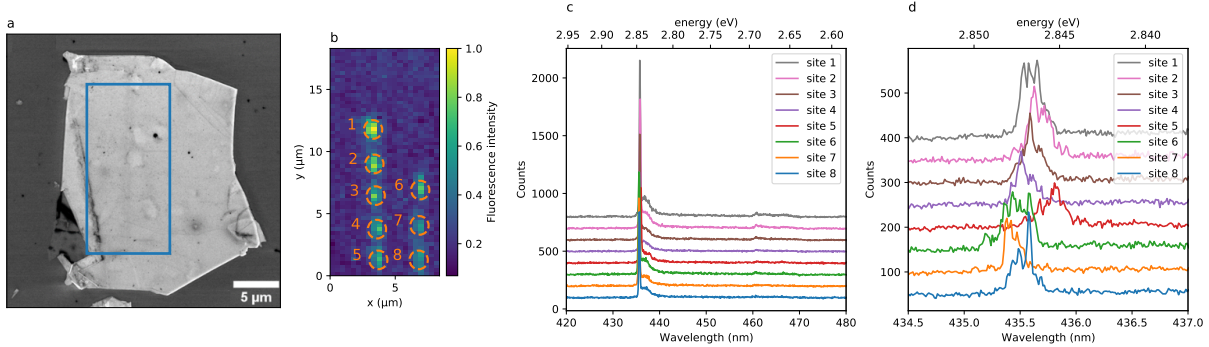
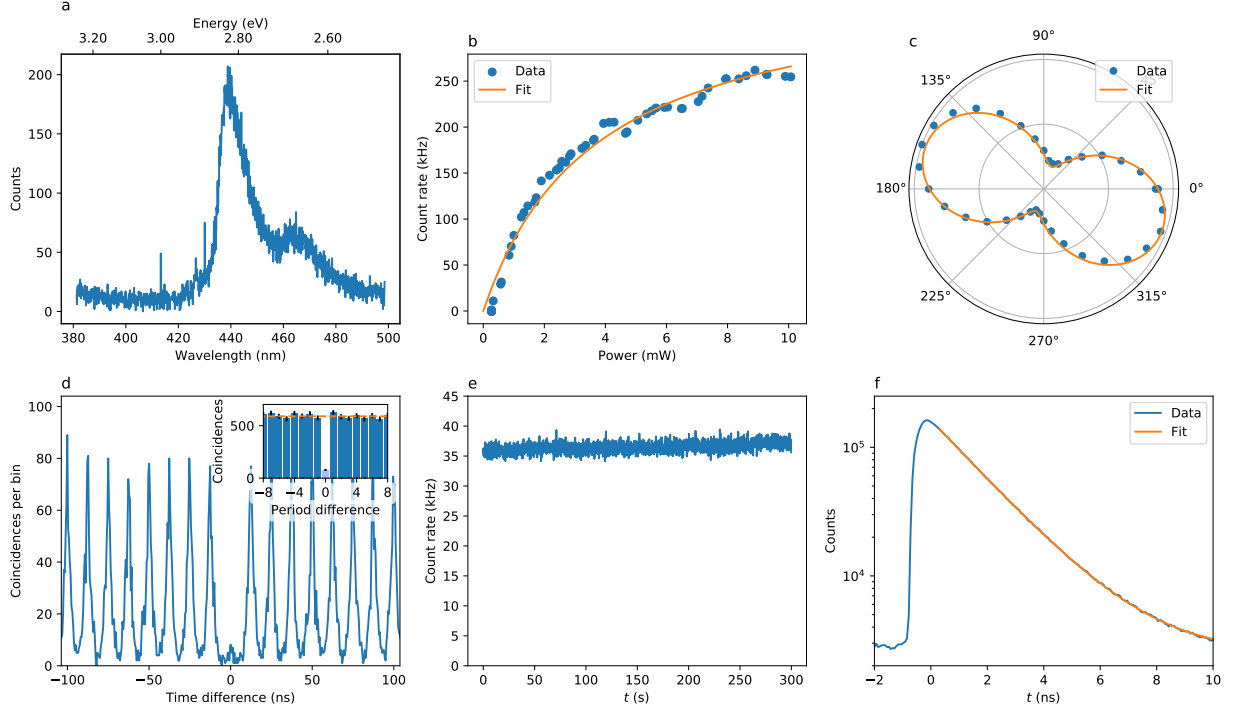


Figure 1. **Activation of localized ensembles of SPEs on a hBN flake.** (a) SEM image of a high-purity hBN flake of about  $15 \times 20 \mu\text{m}$  and 60 nm thickness. (b) Confocal map of the irradiated zone (blue rectangle in Fig. 1a) with eight irradiation spots (orange dashed lines). (c) and (d) Low-temperature spectra of the eight spots with two different spectral resolutions, showing a reproducible ZPL within 0.7 nm.

some of which we could characterize individually (see Supplementary Material). The emitted light is collected by an air objective of NA 0.95, and detected using avalanche photodiodes or a spectrometer (see Methods). Fig. 2 shows the typical room temperature photophysical properties of a single representative colour centre, termed  $\text{SPE}_1$ . The emission spectrum (Fig. 2a) shows that the emission mainly occurs in a ZPL centred at 440 nm, slightly red-shifted as compared with the low temperature emission. An optical phonon replica is visible around 465 nm. Fig. 2b shows the count rate as a function of the laser power. The emission exhibits a saturation behaviour characteristic of two-level systems. We detect up to  $\sim 2.5 \cdot 10^5$  photons per second when the SPE is excited above saturation. We fit the data with the standard power dependence of a two-level system fluorescence  $I(P) = I_{\text{sat}}/(1 + P_{\text{sat}}/P)$ , yielding a saturation power of 3.7 mW and a saturation count rate of 0.36 MHz. This value is limited by the predominant emission of the SPE towards the high index silicon substrate and could be improved by optimized sample design and integration of a photonic structure. Fig. 2c shows the emission polarization data of  $\text{SPE}_1$ . The emission is linearly polarized, suggesting a single dipole transition linearly oriented in the basal plane of the hBN crystal. We have performed second-order correlation measurements in pulsed regime to establish the quantum character of light emitted by  $\text{SPE}_1$ . Fig. 2d shows the results we obtained, with a value of  $g^{(2)}(0) = 0.12 \pm 0.01$  without background correction. This clear antibunching unequivocally demonstrates single photon emission from the colour centre. The count rate is stable over time, as can be observed on Fig. 2e, with no blinking or bleaching observed at timescales  $\geq 1$  ms. Absence

of blinking at shorter timescales is ensured by second order correlations at intermediate timescales (see Supplementary Material). Finally, Fig. 2f shows a fluorescence decay measurement, together with an exponential fit of the data. The lifetime of the excited state is found to be 1.85 ns, of the same order of magnitude as other families of SPEs in hBN.



**Figure 2. Photophysics characterization of an individual SPE at room temperature.** (a) Emission spectrum of SPE<sub>1</sub>, showing a main peak centred at 440 nm (ZPL) and a phonon replica at 465 nm. (b) Count rate as a function of the laser power in cw regime. The orange curve is a fit to the data, from which we extract a saturation power of 3.7 mW and a maximum photon detection rate of  $3.6 \cdot 10^5$  Hz. (c) Count rate as a function of the angle of a polarizer placed before the detector, showing linearly polarized emission. The orange curve is a sine fit of the data. (d) Photon correlations in pulsed regime measured with 315  $\mu$ W excitation power and 80 MHz repetition rate, yielding  $g^{(2)} = 0.12 \pm 0.01$  and thus demonstrating single photon emission. Inset: period-wise integrated coincidences. The dashed orange line denotes the classical limit. (e) Time trace of the photon detection rate with 100 ms binning, calculated from the same raw data as (d). (f) Fluorescence decay in logarithmic scale, extracted from the same raw data as (d). The orange curve is an exponential fit to the data, yielding  $\tau = 1.85$  ns.

We have performed similar measurements on 10 SPEs on two flakes (labelled SPE<sub>1</sub> to SPE<sub>10</sub>). Fig. 3 shows the statistical dispersion of the associated physical quantities. The value of  $g^{(2)}(0)$  (without background correction) is found between 0.1 and 0.25 as shown Fig. 3a, mainly limited

by fluorescence background and emission from nearby SPEs. Fig. 3b shows the statistical spread of the fluorescence lifetime, which is centred around 1.87 ns with a standard deviation of 0.14 ns. Finally, the polarization angle of the emission from 6 SPEs on the same flake, to ensure a common crystalline orientation, is shown Fig. 3c. It exhibits strongly correlated directions: excepted from a single emitter  $\sim 60^\circ$  away, most SPEs emit with approximately the same polarization direction, suggesting a correlation with the crystalline axes. These results shows that the irradiation process yields SPEs with considerably homogeneous properties.

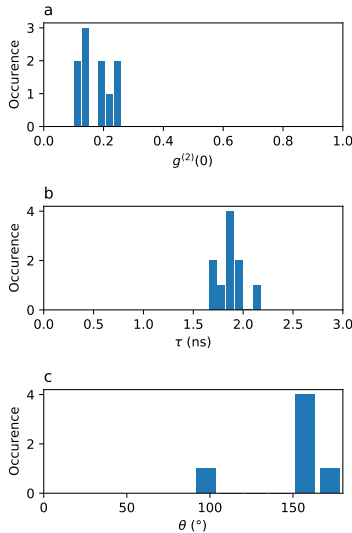


Figure 3. **Statistical dispersion of individual SPE properties.** (a)  $g^{(2)}(0)$  of 10 SPEs, showing single-photon emission. (b) Fluorescence lifetime  $\tau$  of the same 10 individual SPEs, with a mean value of 1.87 ns. (c) Polarization axis of the emission of 6 individual SPEs on the same flake, showing that most SPEs emit with a similar polarization direction.

The spectral properties of individual SPEs at low temperature have been further investigated, and are depicted Fig. 4. For most SPEs, the ZPL linewidth appears to be limited by our spectrometer resolution ( $\sim 150 \mu\text{eV}$ ), which is the case for SPE<sub>1</sub> as shown Fig. 4a. By measuring the emission spectrum as a function of time, we are able to observe the spectral diffusion of the ZPL. Fig. 4b shows the result in the case of SPE<sub>1</sub>. We can observe fluctuations of the centre wavelength at timescales of a few seconds, with a standard deviation of  $45 \mu\text{eV}$ . The spectral diffusion of other SPEs is shown Fig. 4c and d. The standard deviation of the line positions over time typically lies in the range 10 to  $50 \mu\text{eV}$  (2.5 to 12 GHz), although some SPEs with larger fluctuations (a few 100s of  $\mu\text{eV}$ ) have also been encountered. These values are in the very low range of values usually

observed for SPEs in hBN under non-resonant excitation, and could be further improved using resonant excitation [23, 32]. The spectral diffusion, attributed to charge fluctuations in the close environment of the defect, suggests that the emission is sensitive to static electric field, thus opening the way to dc-Stark tuning of the emission line using, for instance, graphene electrodes [33]. Given the natural spectral proximity of the emission from different SPEs, the possibility to electrically tune the emission wavelength could potentially allow to bring any pair of SPEs to resonance, enabling quantum interference of photons emitted by distinct SPEs.

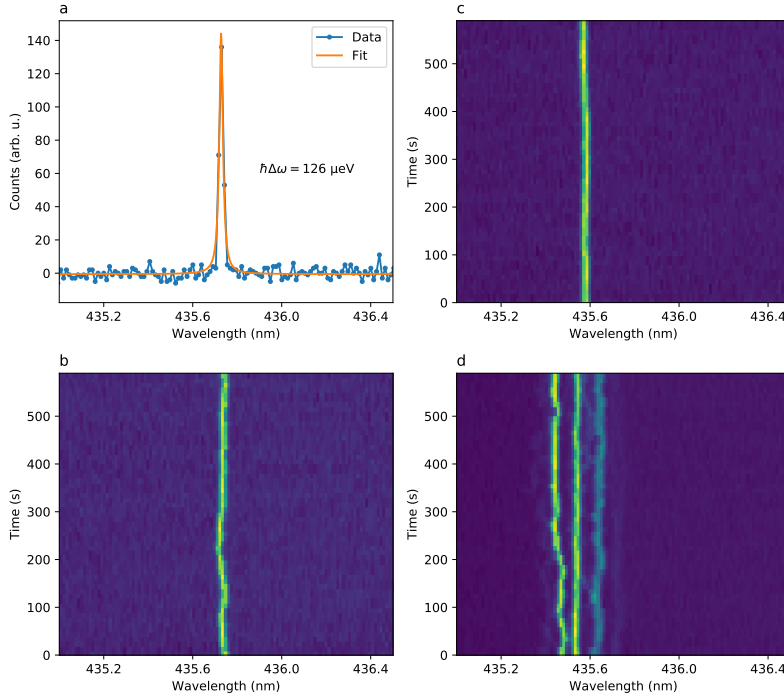


Figure 4. **Spectral properties of individual SPEs at low temperature (5 K).** (a) High-resolution spectrum of SPE<sub>1</sub> ZPL, showing a resolution-limited line at 435.73 nm (b) Spectral diffusion of SPE<sub>1</sub> ZPL during 600 s. The standard deviation of the centre wavelength over time is found to be  $45 \mu\text{eV}$ , as determined by Lorentzian fits of the data. (c) Spectral diffusion of another SPE (SPE<sub>2</sub>) and (d) spectral diffusion of an ensemble of three SPEs, with uncorrelated fluctuations of different magnitudes. All SPEs are excited with 1 mW cw laser light at 405 nm.

In summary, we have demonstrated the possibility to activate SPEs in high-purity hBN at deterministic locations using the electron beam of a commercial SEM. This accessible process is well adapted to potential large-scale or industrial applications. The photophysical properties of the SPEs are advantageous and substantially replicable. In particular, the reproducibility of the

emission line has no equivalent in 2D materials, and could open the way to quantum interference between distinct emitters. Our work brings fundamental questions on the precise nature of the colour centres and on the physical mechanism that renders them optically active upon electron irradiation, that will motivate both further experimental investigations and theoretical studies. On the technological side, it will be desirable to settle methods allowing to deterministically obtain a single SPE per irradiation spot. Such process could for instance make use of in-situ cathodoluminescence measurements [34] during the irradiation process, heralding successful activation of a colour centre. This could in turn enable deterministic coupling of individual SPEs to photonic [35] or plasmonic [36] nanostructures. We expect our research to bring new possibilities to the field of quantum optics in 2D materials, that could yield applications in nanophotonics, integrated quantum optics and quantum information science.

## METHODS

**Sample fabrication.** High-purity hBN was grown under high pressure/high temperature using barium boron nitride ( $\text{Ba}_3\text{B}_2\text{N}_4$ ) as a solvent system. The hBN flakes were obtained by mechanical exfoliation of bulk material on commercial silicon substrates. The SEM imaging and the electron irradiations were performed in a commercial SEM (JEOL 7001F).

**Optical characterization.** For room temperature characterization, the sample was placed in a confocal microscope with an air objective of NA 0.95. Low-temperature characterization was done in a close-cycle cryostat and a low-T objective of NA 0.8 was used. In both cases, the sample was placed on three-axis piezo positioners. A 405 nm laser diode was used to excite the SPEs, either in continuous wave or in pulsed regime (pulse length  $\sim 200$  ps, repetition rate 80 MHz). A dichroic mirror (cutoff wavelength 415 nm) and a fluorescence filter allowed to suppress back-reflected laser light. The signal was fibre-coupled to either a grating spectrometer (Princeton Instruments) or avalanche photodiodes (Micro Photon Devices) with 30 % collection efficiency in the relevant wavelength range, and the detection event were recorded using a time-tagged single photon counting module (PicoQuant). In the photon correlations measurements, only the photons emitted after the laser pulse have been recorded in order to avoid double excitation events caused

by the finite laser pulselength.

---

- [1] Caldwell, J.D., Aharonovich, I., Cassabois, G. *et al.* Photonics with hexagonal boron nitride. *Nat. Rev. Mater.* **4**, 552–567 (2019).
- [2] Atatüre, M., Englund, D., Vamivakas, N. *et al.* Material platforms for spin-based photonic quantum technologies. *Nat. Rev. Mater.* **3**, 38–51 (2018).
- [3] Toth, M. & Aharonovich, I. Single Photon Sources in Atomically Thin Materials. *Annu. Rev. Phys. Chem.* **70**, 123–42 (2019).
- [4] Chakraborty, C., Vamivakas, N. & Englund, D. Advances in quantum light emission from 2D materials. *Nanophotonics* **8**(11), 2017–2032 (2019).
- [5] Geim, A. & Grigorieva, I. Van der Waals heterostructures. *Nature* **499**, 419–425 (2013).
- [6] Castelletto, S., Inam, F. A., Sato, S. & Boretti, A. Hexagonal boron nitride: a review of the emerging material platform for single-photon sources and the spin–photon interface. *Beilstein J. Nanotechnol.* **11**, 740–769 (2020).
- [7] Wang, J., Sciarrino, F., Laing, A. *et al.* Integrated photonic quantum technologies. *Nat. Photonics* **14**, 273–284 (2020).
- [8] Mendelson, N. *et al.* Identifying carbon as the source of visible single-photon emission from hexagonal boron nitride. *Nat. Mater.* (2020).
- [9] Stern, H.L. *et al.* Spectrally Resolved Photodynamics of Individual Emitters in Large-Area Monolayers of Hexagonal Boron Nitride. *ACS Nano* **13**, 4538–4547 (2019).
- [10] Novoselov, K. S., Mishchenko, A., Carvalho, A. & Neto, C. 2D materials and van der Waals heterostructures. *Science* **353**, aac9439 (2016).
- [11] Liu, Y., Weiss, N. O., Duan, X., Cheng, H.-C., Huang, Y. & Duan, X. Van der Waals heterostructures and devices. *Nature Rev. Mater.* **1**, 16042 (2016).
- [12] Aharonovich, I., Englund, D. & Toth, M. Solid-state single-photon emitters. *Nature Photon* **10**, 631–641 (2016).
- [13] Chakraborty, C., Kinnischtzke, L., Goodfellow, K. M., Beams, R. & Vamivakas, A. N. Voltage-controlled quantum light from an atomically thin semiconductor. *Nature Nanotechnol.* **10**, 507–511 (2015).
- [14] He, Y.-M. *et al.* Single quantum emitters in monolayer semiconductors. *Nature Nanotechnol.* **10**, 497–502 (2015).
- [15] Koperski, M. *et al.* Single photon emitters in exfoliated WSe<sub>2</sub> structures. *Nature Nanotechnol.* **10**, 503–506 (2015).
- [16] Srivastava, A. *et al.* Optically active quantum dots in monolayer WSe<sub>2</sub>. *Nature Nanotechnol.* **10**,

- 491–496 (2015).
- [17] Tran, T. T., Bray, K., Ford, M. J., Toth, M. & Aharonovich, I. Quantum emission from hexagonal boron nitride monolayers. *Nat. Nanotechnol.* **11**, 37–41 (2016).
- [18] Tawfik, S. A. *et al.* First-principles investigation of quantum emission from hBN defects. *Nanoscale* **9**, 13575–13582 (2017).
- [19] Abdi, M., Chou, J.-P., Gali, A. & Plenio, M. B. Color centers in hexagonal boron nitride monolayers: a group theory and ab initio analysis. *ACS Photonics* **5**, 1967–1976 (2018).
- [20] Martínez, L. J., Pelini, T., Waselowski, V., Maze, J. R., Gil, B., Cassabois, G. & Jacques, V. Efficient single photon emission from a high-purity hexagonal boron nitride crystal. *Phys. Rev. B* **94**, 121405(R) (2016).
- [21] Chejanovsky, N. *et al.* Structural Attributes and Photodynamics of Visible Spectrum Quantum Emitters in Hexagonal Boron Nitride. *Nano Lett.* **16**, 11, 7037–7045 (2016).
- [22] Li, X. *et al.* Nonmagnetic Quantum Emitters in Boron Nitride with Ultranarrow and Sideband-Free Emission Spectra. *ACS Nano*, **11**, 7, 6652–6660 (2017).
- [23] Dietrich, A. *et al.* Observation of Fourier transform limited lines in hexagonal boron nitride. *Phys. rev. B* **98**, 081414(R) (2018).
- [24] Kianinia M., Regan B., Tawfik, S. A. *et al.* Robust solid-state quantum system operating at 800 K. *ACS Photonics* **4**, 768–73 (2017).
- [25] Tran, T. T. *et al.* Robust Multicolor Single Photon Emission from Point Defects in Hexagonal Boron Nitride. *ACS Nano* **10**, 8, 7331–7338 (2016).
- [26] Choi, S. *et al.* Engineering and Localization of Quantum Emitters in Large Hexagonal Boron Nitride Layers. *ACS Appl. Mater. Interfaces* **8**, 43, 29642–29648 (2016).
- [27] Ziegler, J. *et al.* Deterministic Quantum Emitter Formation in Hexagonal Boron Nitride via Controlled Edge Creation. *Nano Lett.* **19**, 2121–2127 (2019).
- [28] Proscia, N. V. *et al.* Near-deterministic activation of room-temperature quantum emitters in hexagonal boron nitride. *Optica* **5**, 9, 1128–1134 (2018).
- [29] Duong, H. N. M. *et al.* Effects of high energy electron irradiation on quantum emitters in hexagonal boron nitride. *ACS Appl. Mater. Interfaces* **10**, 29, 24886–24891 (2018).
- [30] Taniguchi, T. & Watanabe, K. Synthesis of high-purity boron nitride single crystals under high pressure by using Ba–BN solvent. *J. Cryst. Growth* **303**, 525–529 (2007).
- [31] Shevitski, B. *et al.* Blue-light-emitting color centers in high-quality hexagonal boron nitride. *Phys. Rev. B* **100**, 155419 (2019).
- [32] Konthasinghe, K. *et al.* Rabi oscillations and resonance fluorescence from a single hexagonal boron nitride quantum emitter. *Optica*
- [33] Noh, G. *et al.* Stark Tuning of Single-Photon Emitters in Hexagonal Boron Nitride. *Nano Lett.* **18**,

- 4710-4715 (2018).
- [34] Schué, L. *et al.* Bright Luminescence from Indirect and Strongly Bound Excitons in h-BN. *Phys. Rev. Lett.* **122**, 067401 (2019).
- [35] Kim, S., Fröch, J.E., Christian, J. *et al.* Photonic crystal cavities from hexagonal boron nitride. *Nat. Commun.* **9**, 2623 (2018).
- [36] Tran, T. T., Wang, D., Xu, Z.-Q., Yang, A., Toth, M., Odom, T. W., & Aharonovich, I. Deterministic Coupling of Quantum Emitters in 2D Materials to Plasmonic Nanocavity Arrays. *Nano Lett.* **17**(4), 2634–2639 (2017).

**Supplementary Information** is linked to the online version of the paper

**Acknowledgements** The Authors acknowledge many useful discussions with Christophe Arnold, and Christèle Vilar for technical support on electron microscopy. This work is supported by funding from the French Institute of Physics (INP), and from the French national research agency (ANR) under grant agreement No ANR-14-CE08-0018 (GoBN: Graphene on Boron Nitride Technology). This work also received funding from the European Union’s Horizon 2020 research and innovation program under Grant Nos. 785219 (Graphene Flagship core 2) and 881603 (Graphene Flagship core 3). K.W. and T.T. acknowledge support from the Elemental Strategy Initiative conducted by the MEXT, Japan, Grant Number JPMXP0112101001, JSPS KAKENHI Grant Number JP20H00354 and the CREST (JPMJCR15F3), JST.

**Author Contributions** K.W. and T.T. grew the hBN. Au.P. and M.R. fabricated the samples. Al.P., S.R. and J.B. designed the irradiation protocol and performed the irradiations. C.F. and A.D. performed the optical measurements. S.B., X.Q., J.P.H. and A.D. designed the optical experiments and discussed the data. A.D. supervised the project and wrote the paper, with input from all authors.